Molecular Cancer Therapeutics

Therapeutic Targeting of miR-29b/HDAC4 Epigenetic Loop in Multiple Myeloma

Nicola Amodio[1], Maria Angelica Stamato[1], Anna Maria Gullà[1], Eugenio Morelli[1], Enrica Romeo[1], Lavinia Raimondi[2], Maria Rita Pitari[1], Ida Ferrandino[3], Gabriella Misso[4], Michele Caraglia[4], Ida Perrotta[5], Antonino Neri[6], Mariateresa Fulciniti[7], Christian Rolfo[8], Kenneth C. Anderson[7], Nikhil C. Munshi[7,9], Pierosandro Tagliaferri[1], and Pierfrancesco Tassone[1,10]

Abstract

Epigenetic abnormalities are common in hematologic malignancies, including multiple myeloma, and their effects can be efficiently counteracted by a class of tumor suppressor miRNAs, named epi-miRNAs. Given the oncogenic role of histone deacetylases (HDAC) in multiple myeloma, we investigated whether their activity could be antagonized by miR-29b, a well-established epi-miRNA. We demonstrated here that miR-29b specifically targets HDAC4 and highlighted that both molecules are involved in a functional loop. In fact, silencing of HDAC4 by shRNAs inhibited multiple myeloma cell survival and migration and triggered apoptosis and autophagy, along with the induction of miR-29b expression by promoter hyperacetylation, leading to the downregulation of prosurvival miR-29b targets (SP1, MCL-1). Moreover, treatment with the pan-HDAC inhibitor SAHA upregulated miR-29b, overcoming the negative control exerted by HDAC4. Importantly, overexpression or inhibition of miR-29b, respectively, potentiated or antagonized SAHA activity on multiple myeloma cells, as also shown *in vivo* by a strong synergism between miR-29b synthetic mimics and SAHA in a murine xenograft model of human multiple myeloma. Altogether, our results shed light on a novel epigenetic circuitry regulating multiple myeloma cell growth and survival and open new avenues for miR-29b–based epi-therapeutic approaches in the treatment of this malignancy. *Mol Cancer Ther; 15(6); 1364–75. ©2016 AACR.*

Introduction

Multiple myeloma is a plasma cell malignancy characterized by a high genetic complexity and molecular heterogeneity (1). A number of epigenetic modifications have been so far linked to cancer, including posttranslational modification of histones, DNA methylation, and the most recently discovered noncoding RNAs, which are currently considered key determinants in human cancer pathogenesis (2). In the last few years, a wealth of studies has shown deep dysregulation of miRNAs in human cancers, including multiple myeloma (3). Importantly, replacement of downregulated tumor suppressor (TS) miRNAs (4, 5) or inhibition of oncogenic miRNAs (6–8) have demonstrated therapeutic value in multiple myeloma preclinical settings. A subclass of TS-miRNAs, named epi-miRNAs, is emerging as novel epigenetic regulators, which target and downregulate the expression of DNA methyltransferases (DNMT), histone deacetylases (HDAC), or components of the polycomb repressor complexes, thus representing relevant tools to revert epigenetic aberrations. Among epi-miRNAs, increasing evidence indicates a pivotal role for miR-29b in counteracting *de novo* DNMT expression and in reactivating promoter-hypermethylated TS genes (9–11).

HDACs, key enzymes regulating the acetylation status of both histone- and non-histone proteins, are classified into 4 classes: class I (HDAC1, 2, 3, 8), class IIa (HDAC4, 5, 7, 9) and class IIb (HDAC6,10), class-III (SIRT1-7), and class-IV (HDAC11; ref. 12). Early studies showed that HDACs influenced the expression of several genes involved in cancer initiation and progression. Overexpression of HDACs promotes invasion, migration, angiogenesis, decreased adhesion, and apoptosis in cancer cells (13); therefore, inhibition of HDACs has emerged as a novel treatment strategy in multiple myeloma (14) and other cancers (15, 16). Several HDAC inhibitors (HDACi) are currently in clinical development in multiple myeloma (14, 17–19) and other malignancies,

[1]Department of Experimental and Clinical Medicine, Magna Graecia University and Translational Medical Oncology Unit, Salvatore Venuta University Campus, Catanzaro, Italy. [2]Laboratory of Tissue Engineering - Innovative Technology Platforms for Tissue Engineering (PON01-00829), Rizzoli Orthopedic Institute, Palermo, Italy. [3]Department of Biology, University "Federico II" of Naples, Naples, Italy. [4]Department of Biochemistry, Biophysics and General Pathology, Second University of Naples, Naples, Italy. [5]Department of Biology, Ecology and Earth Sciences (Di.B.E.S.T.), Transmission Electron Microscopy Laboratory, Centre for Microscopy and Microanalysis (CM2), University of Calabria, Rende, Italy. [6]Department of Medical Sciences, University of Milan, Hematology 1, IRCCS Policlinico Foundation, Milan, Italy. [7]Jerome Lipper Multiple Myeloma Center, Department of Medical Oncology, Dana-Farber Cancer Institute, Boston, Massachusetts. [8]Oncology Department, Antwerp University Hospital (UZA) and Center for Oncological Research (CORE) Antwerp University, Antwerp, Belgium. [9]VA Boston Healthcare System, West Roxbury, Boston, Massachusetts. [10]Sbarro Institute for Cancer Research and Molecular Medicine, Center for Biotechnology, College of Science and Technology, Temple University, Philadelphia, Pennsylvania.

Note: Supplementary data for this article are available at Molecular Cancer Therapeutics Online (http://mct.aacrjournals.org/).

M.A. Stamato and A.M. Gullà contributed equally to this article.

Corresponding Authors: Pierfrancesco Tassone, Magna Graecia University and Translational Medical Oncology Unit, Catanzaro 88100, Italy. Phone: 3909-6136-47029; Fax: 3909-6136-47341; E-mail: tassone@unicz.it; and Nicola Amodio, amodio@unicz.it

doi: 10.1158/1535-7163.MCT-15-0985-T

©2016 American Association for Cancer Research.

and specifically vorinostat (SAHA) and romidepsin (FK228 or FR901228) have been FDA approved for the treatment cutaneous T-cell lymphoma, whereas panobinostat was recently approved for multiple myeloma treatment (20, 21). Importantly, many clinical trials using pan-HDACi combined with bortezomib or other anti–multiple myeloma agents have been carried out or are still ongoing, showing encouraging activity of HDACi-based combination regimens in multiple myeloma (22, 23).

We here evaluated the effectiveness of miR-29b in counteracting aberrant HDAC activity and whether its expression might be in turn controlled through acetylation in multiple myeloma. Moreover, the ability of synthetic miR-29b mimics to enhance the anti–multiple myeloma activity of SAHA was investigated in preclinical models of multiple myeloma. We can anticipate that our findings strengthen the central role of miR-29b as an epigenetic modulator and provide the rationale for novel miR-29b–based epi-therapeutic approaches in multiple myeloma.

Materials and Methods

Multiple myeloma cell lines, primary cells, and reagents

Peripheral blood mononuclear cells (PBMC), bone marrow mononuclear cells (BMMNC), and primary cells from multiple myeloma patient bone marrow aspirates, following informed consent and University Magna Graecia (Catanzaro, Italy) IRB approval, were isolated using Ficoll–Hypaque density gradient sedimentation as reported previously (4). Multiple myeloma patient cells were separated from bone marrow samples by antibody-mediated selection using anti-CD138 magnetic-activated cell separation microbeads (Miltenyi Biotec). Multiple myeloma cell lines NCI-H929, RPMI-8226, U266 SKMM1, and MM1s were purchased from DSMZ, which certified authentication performed by short tandem repeat DNA typing. KMS11, KMS12, and KMS34 cells were obtained by the Japanese Collection of Research Bioresources (National Institute of Health Sciences, Japan); OPM2 were kindly provided by Dr. Edward Thompson (University of Texas Medical Branch, Galveston, TX). All these cell lines were immediately frozen and used from the original stock within 6 months. Multiple myeloma cell lines were cultured in RPMI1640 (Gibco, Life Technologies) supplemented with 10% (or 20% for KMS11) FBS (Lonza Group). INA-6 cell line (kindly provided by Dr. Renate Burger, University of Erlangen-Nuernberg, Germany) was cultured in the presence of recombinant human IL6 (25 ng/mL); this cell line was not further authenticated but confirmed for the described IL6 dependence.

Vorinostat (SAHA) was purchased from Selleckchem and dissolved in DMSO. The EpiQuik HDAC4 Assay Kit (colorimetric) was from EpiGentek.

Virus generation, infection, and transfection of multiple myeloma cells

The human HDAC4 (NM_006037.3) mission shRNA set (Sigma Aldrich) and the mission nontarget control (SHC002V; Sigma) were used to generate lentiviral particles as described previously (4). To generate HDAC4-encoding retrovirus, 293Ta cells were cotransfected with 10 μg of pBABEpuro-HDAC4 (kindly provided by Dr. Cécile Haumaitre, INSERM, Paris), 10 μg of pCMV-VSVG, and 4 μg of PEQ-PAM; supernatants were collected 48 hours after 293Ta transfection and used to transduce multiple myeloma cells by three rounds of infection (8 hours each round). Multiple myeloma cells were then selected in medium containing 0.5 μg/mL puromycin. Multiple myeloma cells stably expressing antagomiR-29b were obtained as reported previously (4). Transfection of multiple myeloma cells with synthetic miRNA mimics (Ambion, Applied Biosystems, Life Technologies) was performed using the Neon Transfection System (Invitrogen, Life Technologies) at the following conditions: 2 pulses at 1.050 V, 30 milliseconds.

RNA extraction and quantitative real-time amplification of miRNAs and mRNAs

Total RNA extraction from multiple myeloma cells and qRT-PCR were performed as described previously (4).

Protein extraction and Western blot analysis

Protein lysates and Western blot analysis were performed as reported previously (4) using the anti-HDAC1, anti-HDAC2, anti-HDAC4, anti-HDAC6, anti-acetyl-histone H4 (Lys 8), anti-caspase-3, and anti-caspase-7 antibodies (Cell Signaling Technology); or the anti-SP1, anti-MCL-1, anti-GAPDH, and anti-γ-tubulin antibodies (Santa Cruz Biotechnology). Anti-acetylated α-tubulin antibody was from Abcam.

Chromatin immunoprecipitation

For chromatin immunoprecipitation (ChIP) experiments, the ChIP Assay Kit (Pierce Agarose ChIP Thermo Fisher Scientific) was used. Cells (1.5×10^7) were crosslinked in 1% formaldehyde, lysed, and sheared by sonication for 10 cycles (each of 30 seconds) on a cold block with 90 seconds time intervals of cooling using the Bioruptor Plus (Diagenode). Chromatin was divided into equal amounts for immunoprecipitation with the histone H4 (acetyl Lys 5, 8,12,16) antibody (Thermo Fisher Scientific, PA1-84526) or rabbit anti-IgG as negative control (Santa Cruz Biotechnology). Chromatin extracts were incubated on a rotator with 20 μL of ChIP Grade Protein A/G Plus Agarose for 3 hours at 4°C. Bound agarose beads were harvested by centrifugation (14,000 × *g* for 15 seconds) and washed; the precipitated protein–DNA complexes were then eluted from the washed beads and incubated twice at 65°C for 30 minutes with shaking. Bound DNA was incubated at 65°C for 1.5 hours with NaCl and Proteinase K to revert cross-linking. Purified DNA was subjected to qRT-PCR using GoTaq qPCR Master Mix (Promega). The sequence of PCR primers of miR-29a/b-1 promoter were as follows: Fw, 5′ CATGCCTGTAGTGAGGCTGA 3′; Rev, 5′ TCCTGAGTAGCTGGGATTGC 3′.

Luciferase reporter experiments

The pGL3 luciferase plasmid containing the miR-29a/b1 promoter (nts: −1530 +165) was a gift from Dr. J Mott (University of Nebraska Medical Center, Omaha, NE); *Renilla* luciferase from pCMV-RL was included to normalize firefly luciferase activity. The 3′ untranslated region (UTR) of HDAC4 was cloned in pEZX-MT01 vector and purchased from GeneCopoeia (Rockville, MD). Multiple myeloma cells were electroporated using 2.5 μg of the firefly luciferase reporter; for each plate, 200 nmol/L of the synthetic miR-29b or miR-NC and 0.5 μg of pCMV-RL were used. Firefly and *Renilla* luciferase activities were measured using the Dual-Luciferase Assay Kit (Promega). Data are expressed as the ratio of luminescence from firefly divided by luminescence from *Renilla* luciferase.

Analysis of autophagy

Autophagy was explored by Western blot analysis of LC3A, LC3B, beclin-1, SQSTM1/p62, and TFEB (all from Cell Signaling Technology), by Cyto-ID autophagy detection flow cytometry assay (Enzo Life Sciences) and by ultrastructural analysis with transmission electron microscopy (TEM). For TEM analysis, cells were washed with PBS 1× and then fixed in 2.5% glutaraldehyde in PBS 1× for 2 hours at 4°C. After 4 PBS washings, cells were postfixed in 1% osmium tetroxide for 1 hour, dehydrated in graded ethanol for 90 minutes, and then enclosed in Epon 812. Ultrathin sections were collected on nickel grids and stained with 2% uranyl acetate and 0.65% lead citrate for 7 minutes. TEM observations were carried out at the Anton Dohrn Zoological Station of Naples (Naples, Italy) with a Leo 912 AB electron microscope.

Analysis of cell viability, apoptosis, and cell migration

Cell viability was analyzed by Cell Titer-Glo (Promega); caspase activity was measured using Caspase-Glo 3/7 Assay (Promega). Apoptosis was evaluated by flow cytometric (FACS) analysis following Annexin V-7AAD staining (BD Pharmingen). Cell migration was analyzed by transwell migration assays, as previously reported (10).

In vivo model of human multiple myeloma

Male CB-17 SCID mice (6- to 8 weeks old; Harlan Laboratories, Inc.) were housed and monitored in our Animal Research Facility. All experimental procedures and protocols were approved by our Institutional Ethical Committee and conducted according to the protocols approved by the National Directorate of Veterinary Services. In accordance with institutional guidelines, mice were killed when their tumors reached 2 cm in diameter or in the event of paralysis or major compromise in their quality of life. Mice were subcutaneously inoculated with 5.0×10^6 KMS11-GFP cells, and treatment started when palpable tumors became detectable. Tumor sizes were measured every two days in 2 dimensions using a caliper, and volume was calculated using the formula: $V = 0.5 \times a \times b^2$, where a and b are the long and short diameters of the tumor, respectively; tumors of GFP-expressing xenografts were also measured by IVIS Lumina II (Caliper Life Sciences). To achieve an efficient delivery, miR-29b or scrambled oligonucleotides were formulated using the MaxSuppressor In Vivo LANCEr II (BIoo Scientific). Interaction between miR-29b mimics and SAHA was assessed using the combination index (CI), by the following formula: CI = (inhibition COMBO)/(inhibition miR-29b mimics) + (inhibition SAHA), CI = 1, and CI < 1 indicated synergistic, additive, and antagonistic effects, respectively.

Histology and IHC

Retrieved xenografts were fixed in formalin for 24 hours at 4°C and dehydrated for paraffin embedding. Sections (6 μm) were cut on a microtome, mounted on polylysine-coated glass slides, deparaffinized with xylene, and hydrated with a descending series of ethanol solutions. Antigen retrieval was performed on rehydrated sections with citrate buffer (pH 6.0). After two washings in PBS, primary antibodies were applied at the appropriate dilution (1:100) and then incubated overnight at 4°C. A biotinylated secondary antibody (biotinylated anti-horse IgG, Vector Laboratories, Inc.) was applied at a 1:200 dilution. Immunostains were visualized with an avidin-biotin HRP visualization system (VECTASTAIN ABC Kit). Finally, sections were rinsed with running tap water, dehydrated in alcohol cleared with xylene, and mounted with coverslips using Eukitt Mounting Medium (Calibrated Instruments, Inc.). Negative control sections were similarly treated with omission of the primary antibody. The experiments were repeated at least three times.

Statistical analysis

Each experiment was performed at least 3 times, and values were reported as means ± SD. Comparisons between groups were made with Student *t* test, whereas statistical significance of differences among multiple groups was determined by GraphPad software (www.graphpad.com). $P < 0.05$ was accepted as statistically significant.

Results

HDAC4 is a direct target of miR-29b in multiple myeloma cells

On the basis of the role of miR-29b as epi-miRNA in human cancer, we interrogated microRNA Data Integration Portal, applying the high precision quality filter, to identify HDACs potentially targeted by miR-29b. Among class I, II, and IV HDACs, only the class II HDAC4 was highly predicted as miR-29b target (Supplementary Table S1). To validate the regulation of HDAC4 by miR-29b, we first used the 3′ UTR of HDAC4 cloned into an expression vector downstream of the luciferase reporter gene, which was cotransfected into KMS11 cells together with synthetic miR-29b mimics or scrambled oligonucleotides (NC); levels of miR-29b 24 hours after transfection are shown in Fig. 1A. miR-29b mimics reduced the activity of the reporter but did not regulate the 3′ UTR of HDAC4 devoid of the predicted miR-29b target site (nucleotides 394–417), thus demonstrating that miR-29b specifically regulates HDAC4 mRNA (Fig. 1B). Consistently, transfection of miR-29b mimics into KMS11 cells reduced both HDAC4 mRNA (Fig. 1C) and protein (Fig. 1D) expression but did not affect levels of other HDACs, such as HDAC1, 2, and 6. Importantly, downregulation of HDAC4 was associated to increased acetylation of histone H4 (Fig. 1D) and of α-tubulin (Fig. 1E), suggesting that miR-29b likely regulates the acetylome of multiple myeloma cells via targeting HDAC4. As an additional proof of miR-29b–dependent regulation of HDAC4, we evaluated whether inhibition of miR-29b could upregulate HDAC4 expression. KMS11 cells were stably transduced with a lentiviral vector carrying the antagomiR-29b. Interestingly, miR-29b inhibition led to the upregulation of HDAC4 protein expression, as assessed by Western blotting analysis (Fig. 1F). It was thus possible to conclude that miR-29b is a specific regulator of HDAC4 expression and activity in multiple myeloma cells. Downregulation of HDAC4 by miR-29b along with increased acetylation of both histone H4 and α-tubulin were also demonstrated in SKMM1 cells (Supplementary Fig. S1).

HDAC4 mRNA expression inversely correlates with miR-29b levels in multiple myeloma samples

We next evaluated the expression of HDAC4 mRNA on proprietary datasets of cDNA-microarray of $CD138^+$ cells from multiple myeloma ($n = 55$) or plasma cell leukemia (PCL; $n = 21$) patients and from normal healthy donors plasma cells (PC, $n = 4$). As compared with normal $CD138^+$ cells, PCs from both multiple myeloma and PCL patients expressed higher levels of HDAC4 mRNA (Fig. 2A), suggesting a potential role of this HDAC isoform in the malignant transformation of plasma cells. The

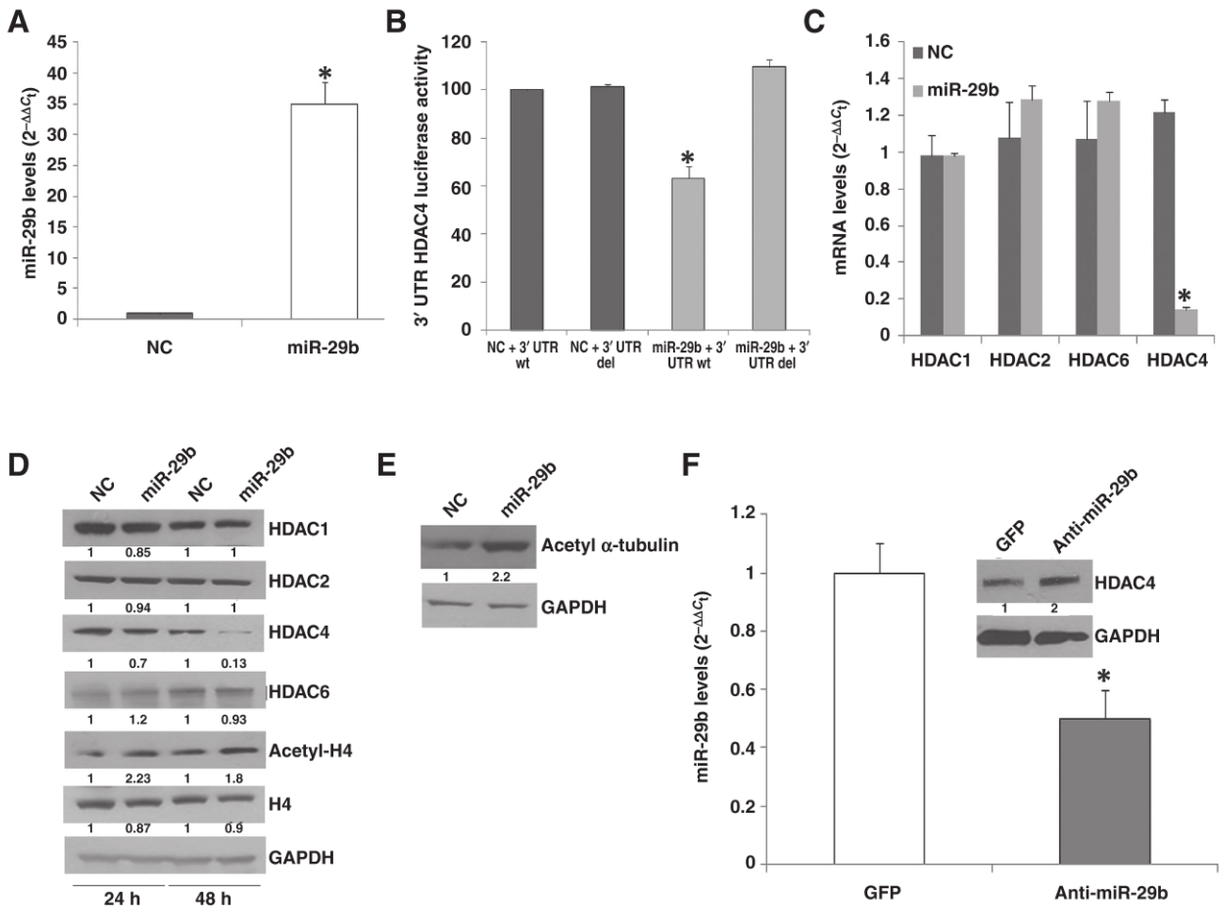

Figure 1.

miR-29b targets HDAC4 in multiple myeloma cells. A, qRT-PCR analysis of miR-29b expression in KMS11 cells 24 hours after transfection with 200 nmol/L miR-29b (miR-29b) or scrambled oligonucleotides (NC). Raw C_t values were normalized to RNU44 housekeeping snoRNA and expressed as $\Delta\Delta C_t$ values; miR-29b levels in NC-transfected cells were set as an internal reference. Data are the average of three independent experiments performed in triplicate. *P* values were obtained using two-tailed *t* test. *, $P < 0.01$. B, dual-luciferase assay of KMS11 cells cotransfected with firefly luciferase constructs containing the 3′ UTR of HDAC4 or a deletion mutant lacking the predicted miR-29b target site (3′ UTR del) and 200 nmol/L of miR-29b or NC as indicated. The firefly luciferase activity was normalized to *Renilla* luciferase activity. The data are shown as relative luciferase activity of miR-29b–transfected cells compared with the control (NC) for a total of six experiments from three independent transfections. *, $P < 0.01$. C, qRT-PCR of HDAC1, HDAC2, HDAC6, and HDAC4 in KMS11 cells, 24 hours after transfection with 200 nmol/L miR-29b or NC. The results are shown as average mRNA expression after normalization with GAPDH and $\Delta\Delta C_t$ calculations. *, $P < 0.01$. D, immunoblot of HDAC1, HDAC2, HDAC4, HDAC6, histone H4, acetyl-histone H4, and GAPDH in SKMM1 transfected with 200 nmol/L miR-29b or NC as indicated. E, immunoblot of acetyl α-tubulin 24 hours after transfection of KMS11 with 200 nmol/L miR-29b or NC. GAPDH was used as loading control. Protein bands were analyzed by ImageJ, and values for NC at each time point were arbitrarily set as 1. F, qRT-PCR of miR-29b in KMS11 cells transduced with the empty vector (carrying GFP) or antagomiR-29b (anti-miR-29b) lentiviral vector. Results are average mRNA expression after normalization with GAPDH. Immunoblot shows the levels of HDAC4 in GFP- or anti-miR-29b–transduced cells. GAPDH was used as a loading control. *, $P < 0.01$. wt, wild type.

analysis by qPCR (Fig. 2B) and Western blot (Fig. 2C) of a panel of 10 multiple myeloma cell lines and primary PCs isolated from multiple myeloma patients confirmed upregulation of HDAC4 both at mRNA and protein levels, as compared with normal healthy donor cells. Moreover, high expression of HDAC4 was associated to increased enzymatic activity in multiple myeloma cell lines compared with control cells (Fig. 2D). Collectively, these findings indicate that both HDAC4 expression and activity are elevated in multiple myeloma cells. Given the direct targeting of HDAC4 by miR-29b (Fig. 1B), we asked whether an inverse correlation between miR-29b and its mRNA target could emerge in multiple myeloma primary samples. The analysis of GSE17306 dataset (24) highlighted a statistically significant inverse correlation ($P = 0.03$; Fig. 2E), thus strengthening the role of miR-29b as HDAC4 negative regulator in multiple myeloma.

Silencing of HDAC4 upregulates miR-29b and phenocopies miR-29b effects in multiple myeloma cells

Given that miRNAs are often involved in feedback loops with their own targets (25), we studied whether miR-29b expression might be under the control of HDAC4 by stably knocking down (KD) HDAC4 with shRNAs cloned into lentiviral vectors. The silencing of HDAC4 caused an increase of miR-29b levels in KMS11, SKMM1, and NCI-H929 cells, assessed by qRT-PCR (Fig. 3A); conversely, ectopic HDAC4 reduced both miR-29b expression (Fig. 3B) and the activity of miR-29a/b1 promoter cloned

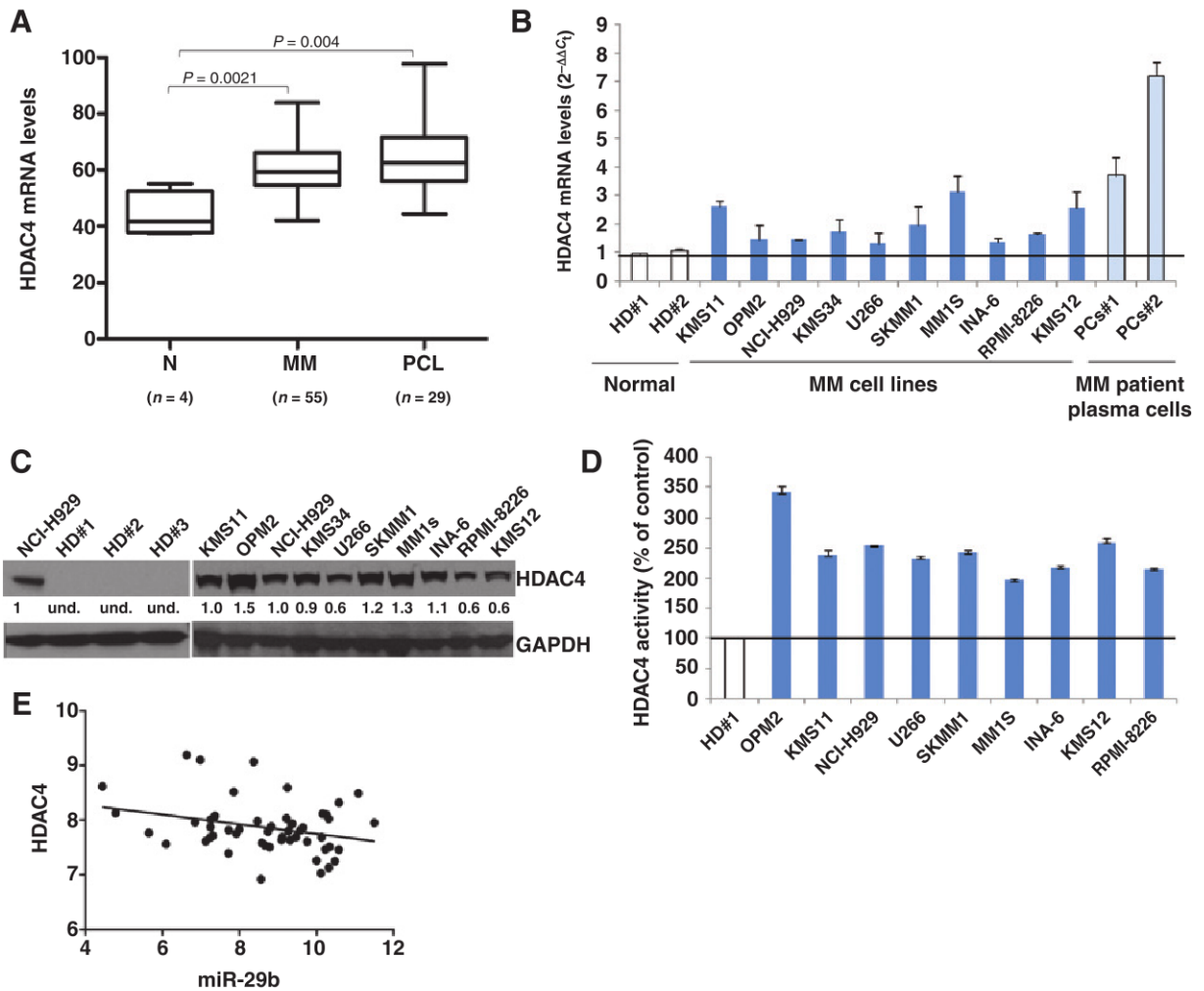

Figure 2.
HDAC4 is overexpressed in multiple myeloma (MM) and its mRNA inversely correlates with miR-29b levels. A, analysis of HDAC4 mRNA levels in patients' multiple myeloma cells from GSE39683 and GSE39925 microarray datasets. N, normal. B, qRT-PCR of HDAC4 in healthy donor PBMCs (HD #1 and HD #2), multiple myeloma cell lines, and patients' multiple myeloma cells (PC #1 and PC #2). Results are shown as average mRNA expression after normalization with GAPDH and $\Delta\Delta C_t$ calculations. HDAC4 levels in HD#1 were set as an internal reference. C, immunoblot of HDAC4 in multiple myeloma cell lines and healthy donor PBMCs (HD). GAPDH was used as a loading control. Protein bands were analyzed by ImageJ, and values for NCI-H929 cells were arbitrarily set as 1. und., undetermined value. D, HDAC4 activity was determined in multiple myeloma cell lines and HD cells as detailed in Materials and Methods. E, inverse correlation between HDAC4 mRNA and miR-29b levels in patients' multiple myeloma cells from dataset GSE17306. Log values of raw data are reported in graph ($P = 0.03$; $R^2 = 0.084$).

upstream the luciferase reporter gene, indicating HDAC4-dependent regulation of miR-29b transcription (Fig. 3C). Interestingly, upregulation of miR-29b triggered by HDAC4 silencing was paralleled by downregulation of miR-29b canonical targets, such as SP1 and MCL-1, and increased acetylation of both histone H4 and α-tubulin (Fig. 3D). To investigate the mechanism by which HDAC4 regulated miR-29b expression, we analyzed the acetylation of histone H4 within miR-29a/b-1 promoter regions by ChIP and found that it was significantly enriched in HDAC4-depleted compared with control cells (Fig. 3E). These results suggest that miR-29b levels are reduced by HDAC4-dependent deacetylation and define a novel negative feedback loop between miR-29b and HDAC4.

We then investigated whether silencing of HDAC4 can mimic the phenotypic changes induced by miR-29b in multiple myeloma cells, such as inhibition of cell survival and migration, as well as induction of apoptosis (4, 9). Silencing of HDAC4 in KMS11, SKMM1, and NCI-H929 cells increased the number of Annexin V–positive cells (Fig. 4A), the percentage of hypodiploid cells determined by FACS (not shown), and caspase-3/7 activity (Fig. 4B), while reduced cell migration in transwell assays (Fig. 4C); moreover, HDAC4 silencing in KMS11 cells enhanced the *in vitro* anti–multiple myeloma activity of dexamethasone, bortezomib, and SAHA (Fig. 4D). HDAC4 overexpression induced by an expression vector lacking the 3′ UTR abrogated the antiproliferative and antimigratory activities triggered by miR-29b mimics (Fig. 4E and F), indicating that miR-29b effects on multiple myeloma cell survival and migration are HDAC4-dependent.

It was reported that HDAC family members play an important role in the modulation of autophagy (26). As HDAC4

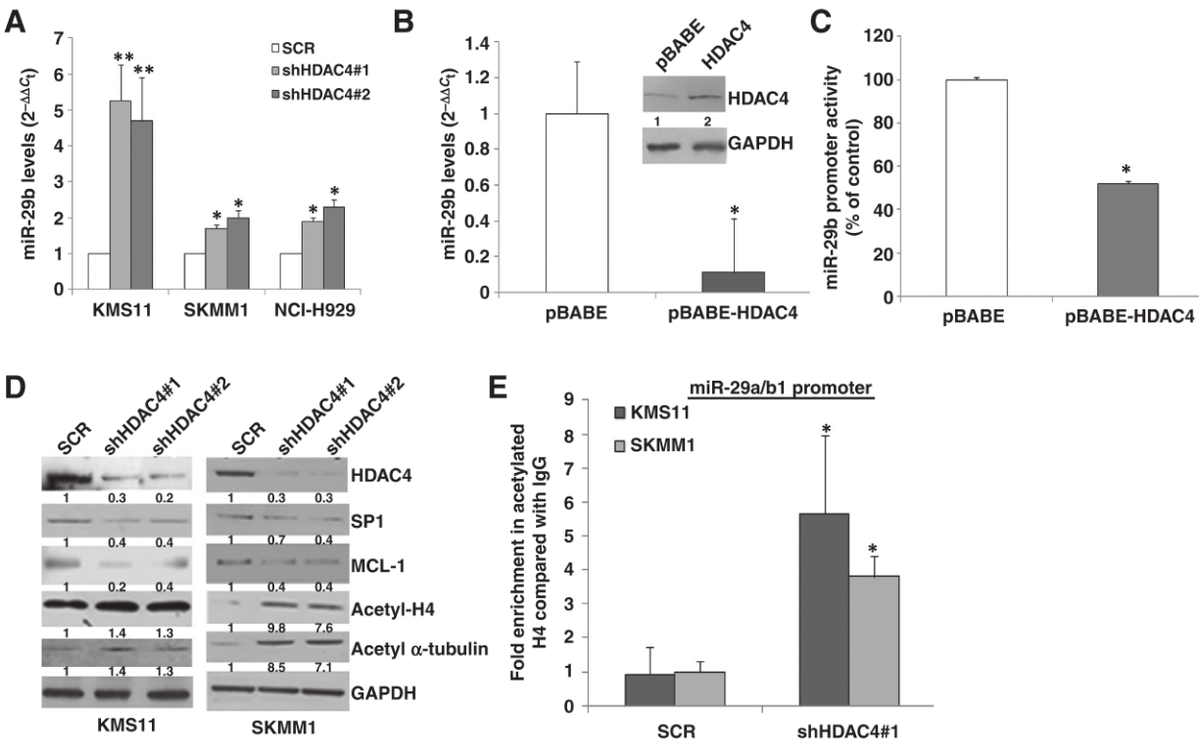

Figure 3.

HDAC4 silencing upregulates miR-29b by promoter hyperacetylation. A, qRT-PCR analysis of miR-29b expression in KMS11, SKMM1, and NCI-H929 cells stably transduced with shRNAs targeting HDAC4 or scrambled (SCR) control. miR-29b levels in SCR-transduced cells were set as internal reference. **, $P < 0.01$; *, $P < 0.05$. B, qRT-PCR analysis of miR-29b expression in KMS11 cells transduced with pBABE or pBABE-HDAC4 retroviruses. miR-29b levels in pBABE-transduced KMS11 cells were set as an internal reference; immunoblot shows the levels of HDAC4 and GAPDH in transduced KMS11 cells. *, $P < 0.05$. C, dual-luciferase assay of KMS11 cells stably expressing HDAC4 or the corresponding empty vector (pBABE) and then transfected with a firefly luciferase construct containing the miR-29a/b1 promoter. *, $P < 0.001$. D, immunoblot analysis of HDAC4, SP1, MCL-1, acetylated histone H4, and acetylated α-tubulin in KMS11 and SKMM1 cells transduced with two different shRNAs targeting HDAC4 or SCR control. GAPDH was used as loading control. E, ChIP assay using an acetylated histone H4 antibody was performed in KMS11 and SKMM1 cells transduced with shRNAs targeting HDAC4 or SCR control. Results are the average of three independent experiments performed in triplicate and show accumulation of acetylated histone H4 on miR-29a/b1 promoter regions of HDAC4-silenced cells. *, $P < 0.05$.

involvement in multiple myeloma autophagic process has not been previously addressed, we first analyzed by TEM the ultrastructural changes induced by stable HDAC4 silencing. Although KMS11 control cells displayed a well-distributed chromatin and a clear nuclear membrane, HDAC4-silenced cells showed several characteristic electron-dense autolysosomes (Fig. 4G). These morphologic features suggest that HDAC4 silencing is involved in autophagy occurrence. Thereafter, we evaluated levels of components of the autophagic machinery or substrates that are degraded by autophagy. Notably, HDAC4-silenced (shHDAC4) cells showed an increase of LC3IIA and LC3IIB, as well as elevated beclin-1, along with decrease in p62/SQSTM1 and in TFEB expression, indicating that HDAC4 inhibits autophagy (Fig. 4H). FACS analysis of Cyto-ID–stained cells revealed an increase of autophagic vacuoles (Supplementary Fig. S2A). Similar effects were observed after transfection with synthetic miR-29b mimics (Supplementary Fig. S2B and S2C). Moreover, exposure of shHDAC4-KMS11 cells to the autophagy inhibitor chloroquine did not revert, rather slightly potentiated, the inhibitory effects on cell survival induced by HDAC4 silencing, thus suggesting that the autophagy elicited by HDAC4-KD does not have a detrimental activity (Supplementary Fig. S2D).

Altogether, these results indicate that HDAC4 is a promising target for therapeutic intervention in multiple myeloma, and its silencing phenocopies miR-29b effects on multiple myeloma cells.

The pan-HDAC inhibitor SAHA upregulates miR-29b in multiple myeloma cells through promoter acetylation

We next investigated whether hyperacetylation-dependent upregulation of miR-29b could also be achieved by pharmacologic means. To this aim, KMS11 and SKMM1 cells were treated with the clinically used pan-HDAC inhibitor SAHA (vorinostat). *In vitro* dose-dependent induction of apoptosis by SAHA on KMS11 and SKMM1 cells (not shown) was paralleled by upregulation of miR-29b, with an optimal effect at 1.0 μmol/L SAHA (Fig. 5A); moreover, 1.0 μmol/L SAHA *ex vivo* treatment of patient multiple myeloma cells also led to miR-29b upregulation (Fig. 5B). Increased miR-29b levels could also be observed in retrieved KMS11 xenografts after systemic treatment with 20 mg/kg SAHA (Fig. 5C). As in shHDAC4 cells, treatment of multiple myeloma cell lines (KMS11, SKMM1, and NCI-H929) with SAHA led to increased acetylation of histone H4 within miR-29a/b1 promoter regions, as assessed by ChIP (Fig. 5D). SAHA-dependent upregulation of miR-29b occurred

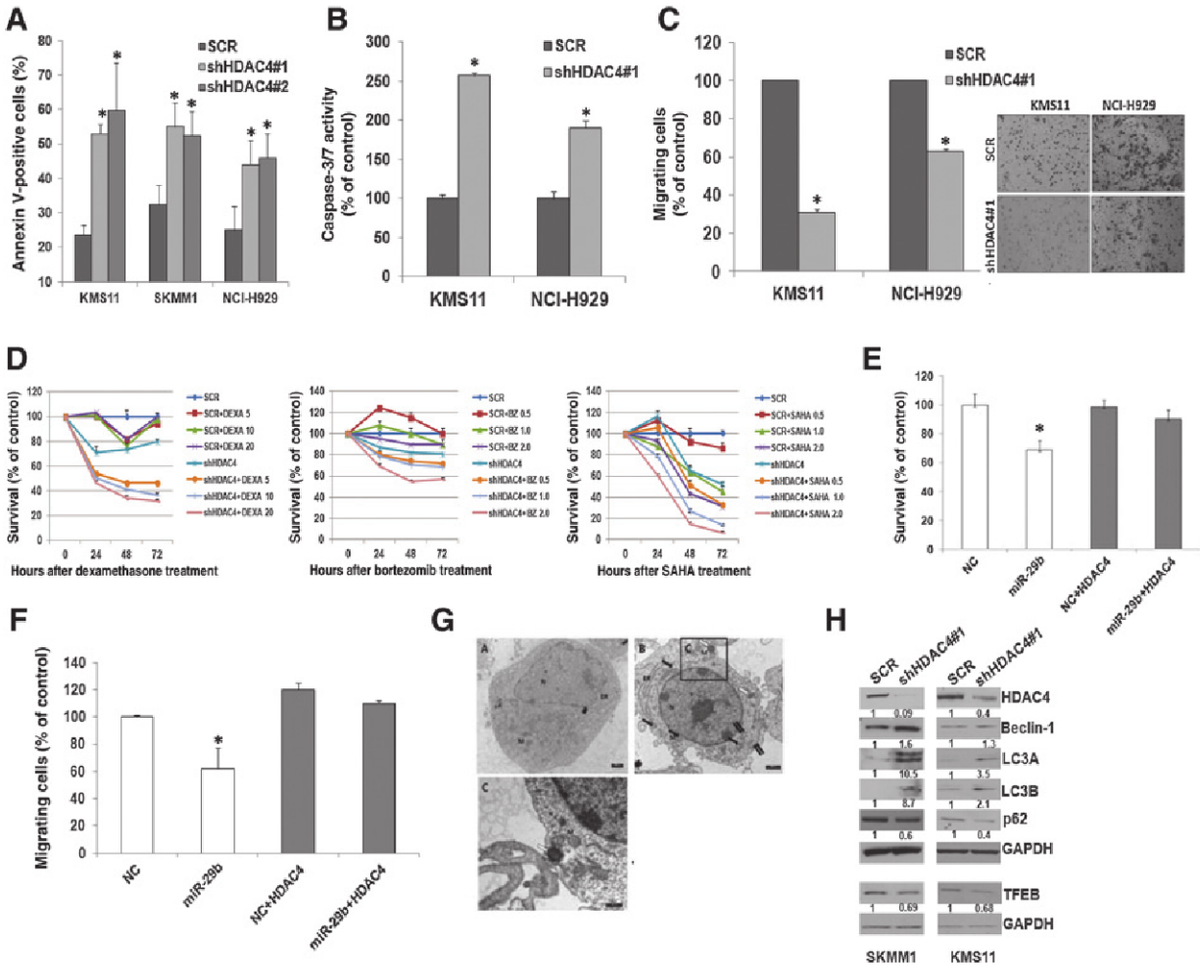

Figure 4.
HDAC4 silencing triggers apoptosis, autophagy, and antimigratory effects in multiple myeloma cells, whereas its overexpression abrogates miR-29b anti–multiple myeloma activity *in vitro*. A, Annexin V staining of KMS11, SKMM1, and NCI-H929 cells stably transduced with shRNAs targeting HDAC4 or scrambled (SCR) control. *, $P < 0.05$. B, caspase-3/7 activity in KMS11 and NCI-H929 cells was determined by Caspase-Glo 3/7 Assay (Promega) according to the manufacturer's instructions; results are average of three independent experiments performed in triplicate. *, $P < 0.05$. C, transwell migration assay of KMS11 and NCI-H929 cells transduced with shRNAs targeting HDAC4 or SCR controls; representative pictures of migrated cells (original magnification, 20×) are shown. D, survival analysis by Cell Titer Glo Assay (Promega) was performed on KMS11 cells stably transduced with shRNAs targeting HDAC4 or SCR controls and then treated with dexamethasone (DEXA) at micromolar concentration, bortezomib (BZ) at nanomolar concentration, or SAHA at micromolar concentration. Results are the average of three independent experiments performed in triplicate; $P < 0.05$ in shHDAC4 cells as compared with SCR cells for each concentration of drug. E, Cell Titer Glo (Promega) survival assay was performed in KMS11 cells stably expressing HDAC4 and analyzed 48 hours after transfection with 200 nmol/L miR-29b mimics or scrambled oligonucleotides (NC). Results are expressed as percentage of NC-transfected cells. *, $P < 0.01$. F, transwell migration assay was performed in KMS11 cells stably expressing HDAC4 and analyzed 48 hours after transfection with 200 nmol/L miR-29b mimics or NC. Results are expressed as percentage of NC-transfected cells. *, $P < 0.01$. G, TEM analysis of SCR-transduced cells (A) and shHDAC4-transduced KMS11 cells (B). C, inset, magnification of shHDAC4-transduced cells (M, mitochondrion; N, nucleus; ER, endoplasmic reticulum; black arrow, double-membrane autophagosomes; double black arrow, phagophore; white arrow, electron-dense autolysosomes; black arrowheads, late autophagic double-membrane vacuoles). H, immunoblot analysis of HDAC4, beclin-1, LC3A, LC3B, p62, and TFEB in SKMM1 and KMS11 cells stably transduced with shRNAs targeting HDAC4 or SCR controls. GAPDH was used as loading control.

together with downregulation of the miR-29b target HDAC4, indicating that SAHA interferes with the miR-29b-HDAC4 loop; in addition, protein levels of other validated miR-29b targets (SP1, MCL-1; ref. 4) were also decreased by SAHA (Fig. 5E). Notably, stable inhibition of miR-29b by antagomiRs abrogated SAHA-dependent downmodulation of HDAC4, SP1, and MCL-1 proteins, indicating that modulation of these targets by SAHA occurred in a miR-29b–dependent manner (Fig. 5F).

miR-29b modulates phenotypic changes triggered by SAHA

As miR-29b is induced by SAHA, we investigated whether the modulation of miR-29b levels affects the response of multiple myeloma cells to the drug. In multiple myeloma cell lines (KMS11, SKMM1, and NCI-H929) treated with SAHA, transfection of miR-29b mimics potentiated the inhibitory effects on cell survival exerted by low drug concentrations (Fig. 6A); moreover, an increased percentage of Annexin V positivity was noted in KMS11 cells transfected with miR-29b mimics and treated with

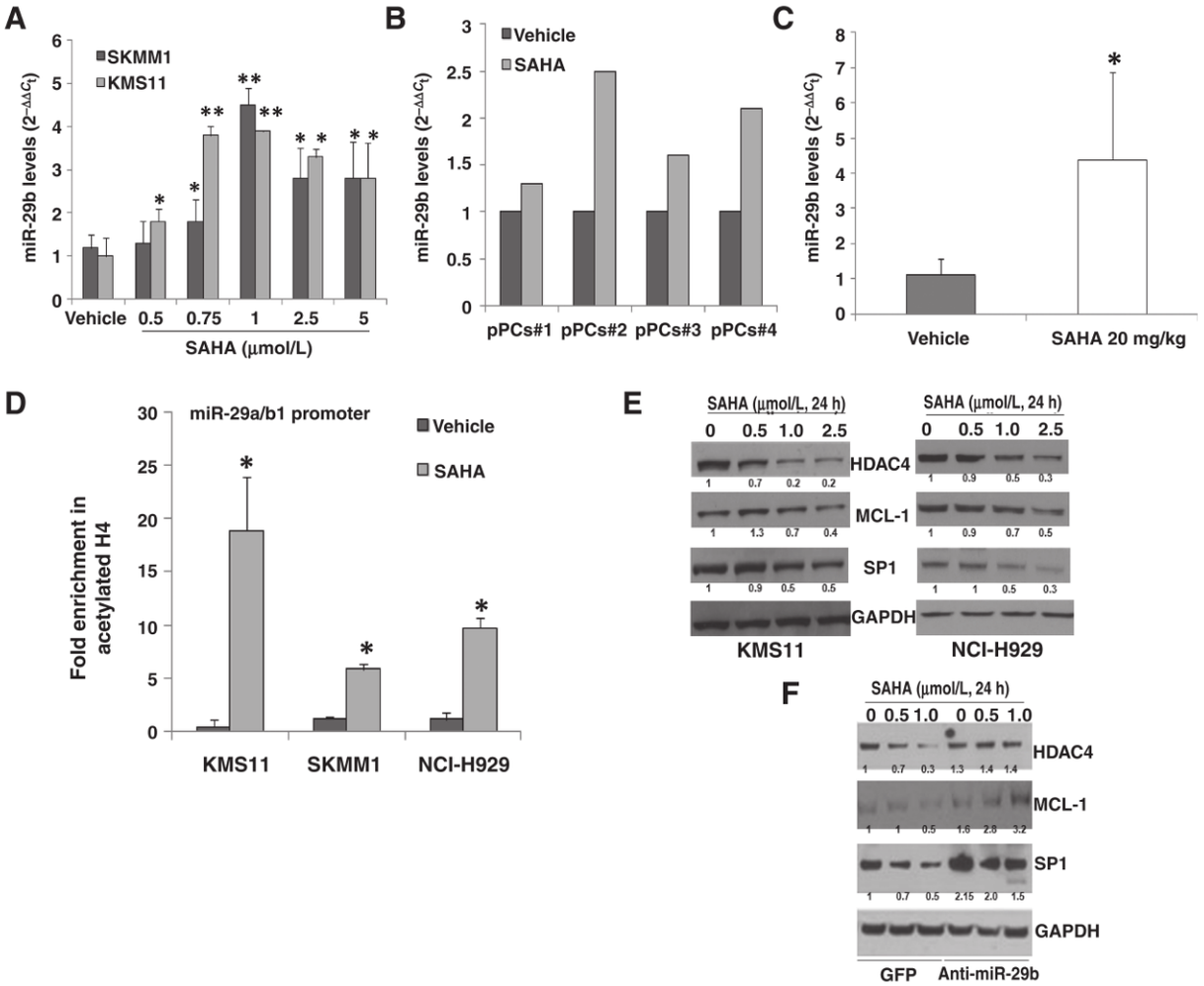

Figure 5.

SAHA upregulates miR-29b and induces miR-29a/b1 promoter hyperacetylation. A, qRT-PCR analysis of miR-29b expression in KMS11 and SKMM1 cells treated for 24 hours with increasing concentrations of SAHA, as reported; miR-29b levels in vehicle-treated cells were set as internal reference. Results are the average of three independent experiments performed in triplicate. *, $P < 0.05$; **, $P < 0.01$ compared with vehicle-treated cells. B, qRT-PCR analysis of miR-29b expression in $CD138^+$ plasma cells isolated from multiple myeloma patients and then treated with 1 μmol/L SAHA for 24 hours. C, miR-29b levels in KMS11 xenografts after treatment with 20 mg/kg SAHA. KMS11-GFP cells (5.0×10^6) were inoculated into the right flank of SCID mice; after the appearance of a palpable tumor, mice were randomized and treated with 20 mg/kg SAHA or vehicle 5 days/week for a total of 4 weeks. Then, mice were sacrificed and miR-29b levels determined in harvested multiple myeloma xenografts by qRT-PCR. Results are the average of three different multiple myeloma xenografts/group. *, $P < 0.01$. D, ChIP assay using an acetylated histone H4 antibody was performed in KMS11, SKMM1, and NCI-H929 cells treated with vehicle or 1.0 μmol/L SAHA for 24 hours. Results are the average of three independent experiments performed in triplicate and show the accumulation of acetylated histone H4 on miR-29a/b1 promoter region of SAHA-treated cells; *, $P < 0.05$. E, immunoblot of HDAC4, SP1, and MCL-1 in KMS11 and NCI-H929 cells treated for 24 hours with increasing concentrations of SAHA. GAPDH was used as a loading control. F, immunoblot of HDAC4, SP1, and MCL-1 in NCI-H929 cells transduced with GFP or anti-miR-29b and then treated for 24 hours with increasing concentrations of SAHA. GAPDH was used as a loading control.

SAHA, as compared with KMS11 cells treated with each agent alone (Supplementary Fig. S3A). Combined miR-29b/SAHA treatments resulted in higher downregulation of miR-29b targets, such as HDAC4 and SP1, activation of caspase-3 and -7, and acetylation of histone H4 (Fig. 6B). To evaluate the effect of miR-29b on the modulation of autophagy caused by SAHA, KMS11 cells transfected with miR-29b mimics and treated with SAHA were analyzed by TEM. Cells transfected with NC appeared intact, with well-distributed chromatin and a clear nuclear membrane, whereas treatment with SAHA led to the accumulation of typical electron-dense autolysosomes, late autophagic double-membrane vacuoles, and characteristic phagophore elongations (Fig. 6C, inset a–d). The analysis of KMS11 and SKMM1 cells by Western blotting confirmed induction of autophagy by SAHA through dose-dependent downregulation of phosphorylated mTOR, the master negative regulator of autophagy, of the autophagy inhibitors TFEB and p62/SQSTM1 and upregulation of beclin-1 and LC3B-II. Increased cleavage of caspase-3 suggests that apoptosis and autophagy occur together in SAHA-treated cells (Supplementary Fig. S3B). KMS11 cells transfected with miR-29b mimics and analyzed by TEM showed several double-membrane autolysosomes and double-membrane autophagosomes

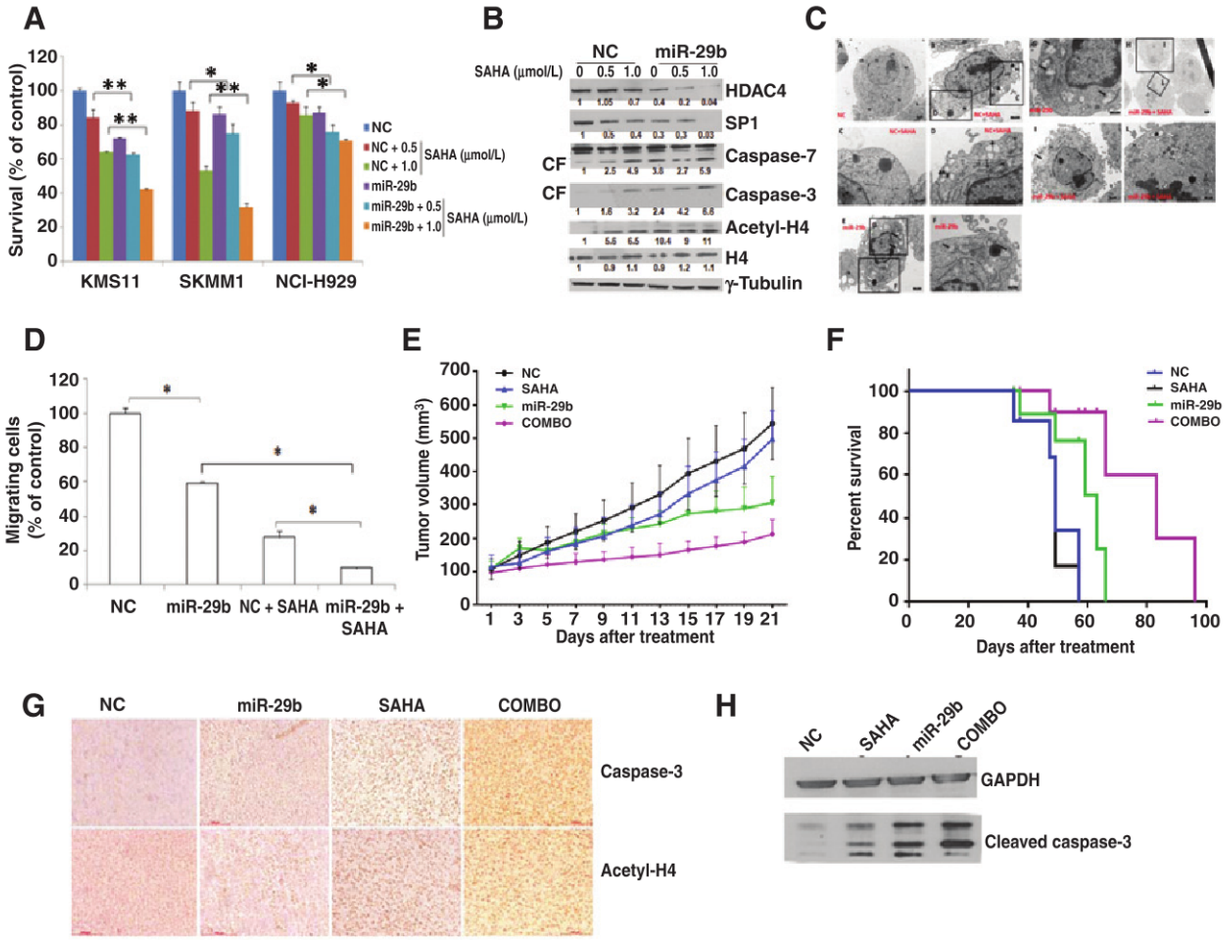

Figure 6.
miR-29b modulates *in vitro* and *in vivo* SAHA activity on multiple myeloma cells. A, KMS11, SKMM1, and NCI-H929 cells were transfected with 200 nmol/L synthetic miR-29b mimics or NC and treated with vehicle or SAHA (0.5 or 1.0 μmol/L) for 48 hours. Survival was assessed by Cell Titer Glo (Promega) and results expressed as percentage of NC-transfected cells. *, $P < 0.05$; **, $P < 0.01$. B, immunoblot analysis of HDAC4, SP1, cleaved form (CF) caspase-3, total and cleaved form caspase-7, acetylated H4, and histone H4 in KMS11 cells transfected with 200 nmol/L miR-29b mimics or NC and treated with SAHA or vehicle for 48 hours. GAPDH was used as a loading control. C, TEM analysis of KMS11 cells transfected with NC (A) or miR-29b mimics 200 nmol/L (E) and treated with 1 μmol/L SAHA for 24 hours (D, H). C, D, F, G, I, L are magnifications (M, mitochondrion; N, nucleus; ER, endoplasmic reticulum; LY, lysosome; black arrow, double-membrane autophagic vesicles; curved arrow, phagophore; white arrow, electron-dense autolysosomes; black arrowheads, late autophagic double-membrane vacuoles; white arrowheads, condensed chromatin). D, transwell migration assay of NCI-H929 transfected with NC or miR-29b mimics (200 nmol/L) and then treated with 0.5 μmol/L SAHA for 24 hours. *, $P < 0.01$. E, average and SE of tumor volume (mm^3) from groups of mice ($n = 6$/group) versus time (days) when tumor was measured. KMS11-GFP cells (5.0×10^6 in 100 μL of serum-free RPMI1640 medium) were implanted in the flank of CB17 SCID mice. After tumor detection, mice were randomized to intraperitoneal treatment with vehicle and SAHA (20 mg/kg) or intratumoral treatment with NC or miR-29b synthetic oligonucleotides (1.0 mg/kg). Mice were treated for 5 days/week over 4 consecutive weeks. A significant decrease in tumor growth was noted in combination (COMBO)-treated mice versus vehicle-treated mice ($P = 0.001$ at day 19; $P = 0.0007$ at day 21) and versus miR-29b–treated mice ($P = 0.01$ at day 19; $P = 0.02$ at day 21). *P* values were obtained using two-tailed *t* test. F, Kaplan–Meier plot showing survival for mice treated with vehicle, SAHA, mir-29b mimics, or their combination. SAHA plus miR-29b mimics–treated mice show significantly increased survival in comparison with vehicle-treated mice. Survival was evaluated from the first day of treatment until death or sacrifice. *P* values were calculated by log-rank test. G, micrographs (magnification, 10×) show tumors sectioned from vehicle-, SAHA-, miR-29b mimics-, or combination-treated mice immunostained for caspase-3 or acetylated histone H4. Photographs are representative of 2 mice receiving each treatment. H, immunoblot of caspase-3 in lysates from a representative KMS11 xenograft per group, harvested at day 21. GAPDH was used as a loading control.

fused with lysosomes to form autolysosomes (Fig. 6C, inset e–g). Importantly, cells transfected with miR-29b and treated with SAHA displayed typical apoptotic changes, including pyknosis and chromatin condensation, confirming the synergistic apoptotic effects triggered by SAHA/miR-29b mimics combination (Fig. 6C, inset h–l). We also analyzed the effects of miR-29b plus low doses of SAHA on the migratory capability of multiple myeloma cells and found that migration was impaired to a greater extent in NCI-H929 cells treated with miR-29b mimics plus SAHA, as compared with each single agent alone (Fig. 6D). We finally assessed whether miR-29b inhibition could dampen the phenotypic changes induced by SAHA. To this purpose, NCI-H929 cells transduced with antagomiR-29b were treated with SAHA and analyzed for apoptosis and cell migration. Notably, miR-29b

inhibition antagonized apoptosis triggered by SAHA, as assessed by caspase-3/7 activity assays (Supplementary Fig. S4A) and caspase-3 cleavage analysis (Supplementary Fig. S4B). Moreover, antimigratory activity of SAHA on NCI-H929 cells was similarly reduced in antagomiR-29b–transduced cells as compared with control cells (Supplementary Fig. S4C). Overall, these results demonstrate that miR-29b contributes to the phenotypic changes induced by SAHA on multiple myeloma cells.

miR-29b mimics plus SAHA trigger inhibition of human multiple myeloma cell growth *in vivo*

Having shown that the modulation of miR-29b levels affects anti–multiple myeloma effects of SAHA *in vitro*, we evaluated, *in vivo*, the efficacy of miR-29b/SAHA–combined treatment using the human plasmacytoma KMS11/GFP xenograft mouse model. As clinical studies have shown that HDAC inhibitors are not effective as single agents, while have shown therapeutic efficacy within combination regimens (23), the combination with miRNAs can be an attractive strategy to implement their activity. For this purpose, we used low doses of intraperitoneally administered SAHA (20 mg/kg 5 days per week, over 4 consecutive weeks) that were previously reported to have minimal effects on human multiple myeloma xenografts (27), combined with subcutaneous (intratumor) neutral lipid emulsion (NLE)–formulated miR-29b mimics (1 mg/kg, same treatment schedule of SAHA). As seen in Fig. 6E, SAHA had minimal effect on tumor growth, whereas NLE-formulated miR-29b mimics reduced tumor growth by about 50%. Importantly, when SAHA was combined with miR-29b mimics, there was a significant reduction in tumor growth as compared with untreated mice or with miR-29b–treated animals ($P < 0.001$ and $P < 0.05$, respectively; CI > 1.0 starting from day 9). A representative IVIS Lumina image of xenografted mice at the end of the treatment is shown in Supplementary Fig. S5. Furthermore, combined treatment was well tolerated without weight loss or neurologic changes (data not shown). The median overall survival of miR-29b/SAHA–treated mice was significantly longer than vehicle-treated mice (96 vs. 57 days; $P = 0.0029$) or mice treated with SAHA (49 days, $P = 0.0051$) or miR-29b mimics alone (66 days, $P = 0.0409$; Fig. 6F). Together, these findings suggest that combining miR-29b mimics with SAHA markedly reduces tumor growth and is well tolerated *in vivo*.

We also examined the effect of this combination treatment *in vivo* by caspase-3 staining of human multiple myeloma xenografts harvested from treated mice. Combination therapy significantly increased the number of cleaved caspase-3–positive multiple myeloma cells as compared with single-agent treatments. A significant increase in the acetylation of histone H4 was also noted in tumor sections from combination-treated mice as compared with mice receiving treatment with either SAHA or NLE–miR-29b mimics alone (Fig. 6G). Moreover, increased caspase-3 cleavage could be observed in lysates from KMS11 xenografts (Fig. 6H). Together, these results demonstrate potent *in vivo* anti–multiple myeloma activity of miR-29b mimics combined with SAHA at doses that are well tolerated, providing the framework for translational development of this combination in the treatment of multiple myeloma patients.

Discussion

A rising body of evidence indicates that epigenetic alterations play a role in the pathogenesis of hematologic malignancies, including multiple myeloma. In this work, we defined a new mean to antagonize multiple myeloma–related epigenetic abnormalities by using epi-miRNAs, a subclass of TS-miRNAs, whose anticancer activity resides in targeting and downregulation of components of the epigenetic machinery (11, 28). As HDACs are aberrantly expressed and play a pivotal role in the pathobiology of multiple myeloma (23), we investigated whether miR-29b, a well-recognized epi-miRNA in hematologic (9, 10, 29, 30) and solid tumors (11, 31), could inhibit HDACs in multiple myeloma.

The basic rationale of our investigation was provided by *in silico* analysis, which allowed to identify HDAC4 as a putative target of miR-29b.

HDAC4 is a part of class II HDACs, enzymes regulating development and differentiation, whose involvement in human diseases has been described (32). In solid tumors (33–36), targeting of HDAC4 was shown to inhibit cell survival, to restore tumor cell sensitivity to chemotherapy (37), and to affect hypoxia (38). Here, we demonstrate that multiple myeloma cells disclose high expression of HDAC4, which results from a negative feedback loop with miR-29b: the inverse correlation between miR-29b and HDAC4 observed in multiple myeloma patients, along with specific mRNA-3′ UTR targeting by miR-29b, indicates that HDAC4 overexpression could rely on the lack of miR-29b–mediated inhibitory activity in low miR-29b–expressing multiple myeloma (4, 39). Importantly, miR-29b mimics downregulated HDAC4, while sparing HDAC1, 2, and 6; furthermore, miR-29b–dependent downmodulation of HDAC4 was paralleled by increased acetylation of both histone H4 and α-tubulin, demonstrating for the first time that miR-29b affects the acetylome of multiple myeloma cells and therefore providing novel information, which widens the role of miR-29b as epi-miRNA.

The potential impact of our results is related to emerging findings on the prognostic weight and potential as therapeutic targets of HDACs in multiple myeloma, as shown by recent work demonstrating a significantly shorter progression-free survival of multiple myeloma patients with higher levels of class I/II HDACs (40); moreover, class II HDAC inhibition was proven to enhance the anti–multiple myeloma activity of ER stressors, such as carfilzomib (41), whereas peptide-mediated disruption of HDAC4/RelB complex was found to block multiple myeloma growth (42). In this light, we here provide novel findings unraveling the molecular and functional role of HDAC4 and its regulation in multiple myeloma cells. Thus far, only a few histone- or protein substrates of HDAC4 have been identified in cancer (32, 37); furthermore, the effect triggered by the HDAC4-dependent deacetylation on the miRNA profile has not been previously described in multiple myeloma cells. Here, we show that stable HDAC4 downregulation by shRNAs led to hyperacetylation of miR-29-a/b1 promoter regions along with increased miR-29b expression and downmodulation of anti-apoptotic or prosurvival miR-29b targets, such as SP1 (4, 43) and MCL-1 (4, 44). Our investigation therefore widens the repertoire of validated HDAC4 targets and indeed demonstrates the involvement of HDAC4 in an epigenetic feedback loop with miR-29b, adding new insights on the epigenetic mechanisms controlling multiple myeloma cell growth and survival. Of note, our data are in agreement with previous reports demonstrating that HDACs mediate the silencing of tumor suppressor miRNAs, including miR-29b, in leukemic cells (45, 46), suggesting that HDAC-dependent downregulation of miR-29b is a common feature in cancer cells.

By analyzing the phenotypic changes associated to HDAC4 silencing in multiple myeloma cells, we found effects mimicking

miR-29b overexpression, that is, induction of apoptosis and inhibition of cell viability and migration (4, 10), which are consistent with HDAC4-dependent upregulation of miR-29b.

On the basis of the above-mentioned findings, we attempted to identify a pharmacologic strategy to reactivate epigenetically silenced miR-29b via HDAC inhibition. With the goal of translating our findings to the clinic, we focused on the pan-HDACi SAHA (vorinostat), an FDA-approved drug for the treatment of cutaneous T-cell lymphoma (20). SAHA, a hybrid polar compound (47) with a longer half-life, lower toxicity, and greater stability than earlier HDACi has demonstrated encouraging activity in patients with relapsed and/or refractory multiple myeloma in combination with novel (carfilzomib, lenalidomide) or conventional (dexamethasone) drugs (22, 48, 49). Molecular mechanisms underlying SAHA activity are diverse and not completely understood. In this work, we showed that SAHA disrupted the miR-29b/HDAC4 loop by promoting miR-29b promoter hyperacetylation and increased expression of miR-29b both in multiple myeloma cell lines and primary multiple myeloma cells. Of note, SAHA triggered apoptosis and autophagy, along with downregulation of miR-29b targets, such as SP1, MCL-1, and HDAC4. Importantly, downmodulation of these targets was abrogated by miR-29b inhibition, the latter finding indicating a novel function of miR-29b as mediator of the molecular effects triggered by SAHA.

We also investigated whether the modulation of miR-29b could affect the anti–multiple myeloma activity induced by SAHA. *In vitro*, synthetic miR-29b mimics were proven to enhance both the inhibition of cell viability and migration, and the induction of apoptosis triggered by low concentration of SAHA, and these effects were dampened by miR-29b inhibition. Interestingly, TEM analysis of multiple myeloma cells treated with miR-29b mimics plus SAHA indicated the accumulation of autophagosomes promoted by each agent alone; conversely, combination treatments led to the appearance of apoptotic markers, such as pyknosis and chromatin condensation.

It is of interest to understand the significance of the autophagy that has been clearly demonstrated in cells exposed to miR-29b mimics or SAHA. Several lines of evidence suggest that there is a cellular stress threshold that dictates the transition from a cytoprotective to a cytotoxic autophagy (50). It is tempting to speculate that the higher cellular stress produced by miR-29b/SAHA combination might lead to cell death, likely overcoming the protective autophagy elicited by SAHA alone and pushing autophagy towards apoptosis. In line with this hypothesis, active caspase-3 and -7 increased, while miR-29b antiapoptotic and prosurvival targets as SP1 and HDAC4 decreased, after cell exposure to miR-29b/SAHA combination at a greater extent as compared with single-agent treatment.

Finally, synthetic miR-29b mimics plus low doses of SAHA triggered *in vivo* synergistic antitumor activity in a murine model of human multiple myeloma in the absence of evident organ toxicity. This evidence provides a framework for clinical development of miR-29b/SAHA combination regimens to improve effectiveness of therapy with HDACi, which have shown neglectable single-agent anti–multiple myeloma activity (22).

In conclusion, our investigation identifies a novel epigenetic microcircuitry involving miR-29b and HDAC4 in multiple myeloma cells and offers the proof of concept that miR-29b–based targeted therapies represent a novel strategy to modulate the epigenome in multiple myeloma.

Disclosure of Potential Conflicts of Interest

No potential conflicts of interest were disclosed.

Authors' Contributions

Conception and design: N. Amodio, C. Rolfo, P. Tagliaferri, P. Tassone
Development of methodology: N. Amodio, L. Raimondi, I. Ferrandino
Acquisition of data (provided animals, acquired and managed patients, provided facilities, etc.): N. Amodio, M.A. Stamato, E. Romeo, M.R. Pitari, G. Misso, A. Neri
Analysis and interpretation of data (e.g., statistical analysis, biostatistics, computational analysis): N. Amodio, A.M. Gullà, E. Morelli, L. Raimondi, I. Ferrandino, G. Misso, M. Caraglia, C. Rolfo, K.C. Anderson, N.C. Munshi, P. Tagliaferri
Writing, review, and/or revision of the manuscript: N. Amodio, M. Caraglia, M. Fulciniti, C. Rolfo, K.C. Anderson, N.C. Munshi, P. Tagliaferri, P. Tassone
Study supervision: N. Amodio, P. Tassone
Other (IHC experiments): I. Perrotta
Other (provided biologic samples): A. Neri

Acknowledgments

The authors thank Stazione Zoologica "Anton Dohrn" and CISME of University of Naples "Federico II" for technical assistance at TEM and Dr. Marzia Leotta for invaluable support at the beginning of the project.

Grant Support

This work has been supported by funds of Italian Association for Cancer Research (AIRC), "Special Program Molecular Clinical Oncology - 5 per mille" n. 9980, 2010/15 (to P. Tassone). This work has also been supported by grants from NIH P01CA155258, P50CA100707, I01BX001584, and P01CA78378 and VA merit grant IO1-24467 (to N.C. Munshi). N. Amodio was supported by a "Fondazione Umberto Veronesi" Post-Doctoral Fellowship.

The costs of publication of this article were defrayed in part by the payment of page charges. This article must therefore be hereby marked *advertisement* in accordance with 18 U.S.C. Section 1734 solely to indicate this fact.

Received December 16, 2015; revised March 16, 2016; accepted March 18, 2016; published OnlineFirst March 28, 2016.

References

1. Bianchi G, Anderson KC. Understanding biology to tackle the disease: Multiple myeloma from bench to bedside, and back. CA Cancer J Clin 2014;64:422–44.
2. Dimopoulos K, Gimsing P, Gronbaek K. The role of epigenetics in the biology of multiple myeloma. Blood Cancer J 2014;4:e207.
3. Ahmad N, Haider S, Jagannathan S, Anaissie E, Driscoll JJ. MicroRNA theragnostics for the clinical management of multiple myeloma. Leukemia 2014;28:732–8.
4. Amodio N, Di Martino MT, Foresta U, Leone E, Lionetti M, Leotta M, et al. miR-29b sensitizes multiple myeloma cells to bortezomib-induced apoptosis through the activation of a feedback loop with the transcription factor Sp1. Cell Death Dis 2012;3:e436.
5. Zhao JJ, Lin J, Zhu D, Wang X, Brooks D, Chen M, et al. miR-30-5p functions as a tumor suppressor and novel therapeutic tool by targeting the oncogenic Wnt/beta-catenin/BCL9 pathway. Cancer Res 2014;74:1801–13.
6. Leone E, Morelli E, Di Martino MT, Amodio N, Foresta U, Gulla A, et al. Targeting miR-21 inhibits in vitro and in vivo multiple myeloma cell growth. Clin Cancer Res 2013;19:2096–106.
7. Leotta M, Biamonte L, Raimondi L, Ronchetti D, Di Martino MT, Botta C, et al. A p53-dependent tumor suppressor network is induced by selective miR-125a-5p inhibition in multiple myeloma cells. J Cell Physiol 2014;229:2106–16.
8. Di Martino MT, Gulla A, Cantafio ME, Lionetti M, Leone E, Amodio N, et al. In vitro and in vivo anti-tumor activity of miR-221/222 inhibitors in multiple myeloma. Oncotarget 2013;4:242–55.

9. Amodio N, Leotta M, Bellizzi D, Di Martino MT, D'Aquila P, Lionetti M, et al. DNA-demethylating and anti-tumor activity of synthetic miR-29b mimics in multiple myeloma. Oncotarget 2012;3:1246–58.
10. Amodio N, Bellizzi D, Leotta M, Raimondi L, Biamonte L, D'Aquila P, et al. miR-29b induces SOCS-1 expression by promoter demethylation and negatively regulates migration of multiple myeloma and endothelial cells. Cell Cycle 2013;12:3650–62.
11. Amodio N, Rossi M, Raimondi L, Pitari MR, Botta C, Tagliaferri P, et al. miR-29s: a family of epi-miRNAs with therapeutic implications in hematologic malignancies. Oncotarget . 2015;6:12837–61.
12. de Ruijter AJ, van Gennip AH, Caron HN, Kemp S, van Kuilenburg AB. Histone deacetylases (HDACs): characterization of the classical HDAC family. Biochem J 2003;370:737–49.
13. Bolden JE, Peart MJ, Johnstone RW. Anticancer activities of histone deacetylase inhibitors. Nat Rev Drug Discov 2006;5:769–84.
14. Hideshima T, Cottini F, Ohguchi H, Jakubikova J, Gorgun G, Mimura N, et al. Rational combination treatment with histone deacetylase inhibitors and immunomodulatory drugs in multiple myeloma. Blood Cancer J 2015;5:e312.
15. Lane AA, Chabner BA. Histone deacetylase inhibitors in cancer therapy. J Clin Oncol 2009;27:5459–68.
16. Quintas-Cardama A, Santos FP, Garcia-Manero G. Histone deacetylase inhibitors for the treatment of myelodysplastic syndrome and acute myeloid leukemia. Leukemia 2011;25:226–35.
17. DeAngelo DJ, Spencer A, Bhalla KN, Prince HM, Fischer T, Kindler T, et al. Phase Ia/II, two-arm, open-label, dose-escalation study of oral panobinostat administered via two dosing schedules in patients with advanced hematologic malignancies. Leukemia 2013;27:1628–36.
18. Ocio EM, Richardson PG, Rajkumar SV, Palumbo A, Mateos MV, Orlowski R, et al. New drugs and novel mechanisms of action in multiple myeloma in 2013: a report from the International Myeloma Working Group (IMWG). Leukemia 2014;28:525–42.
19. Santo L, Hideshima T, Kung AL, Tseng JC, Tamang D, Yang M, et al. Preclinical activity, pharmacodynamic, and pharmacokinetic properties of a selective HDAC6 inhibitor, ACY-1215, in combination with bortezomib in multiple myeloma. Blood 2012;119:2579–89.
20. Zhang QL, Wang L, Zhang YW, Jiang XX, Yang F, Wu WL, et al. The proteasome inhibitor bortezomib interacts synergistically with the histone deacetylase inhibitor suberoylanilide hydroxamic acid to induce T-leukemia/lymphoma cells apoptosis. Leukemia 2009;23:1507–14.
21. Fenichel MP.FDA approves new agent for multiple myeloma. J Natl Cancer Inst 2015;107:djv165.
22. Dimopoulos M, Siegel DS, Lonial S, Qi J, Hajek R, Facon T, et al. Vorinostat or placebo in combination with bortezomib in patients with multiple myeloma (VANTAGE 088): a multicentre, randomised, double-blind study. Lancet Oncol 2013;14:1129–40.
23. Kaufman JL, Fabre C, Lonial S, Richardson PG. Histone deacetylase inhibitors in multiple myeloma: rationale and evidence for their use in combination therapy. Clin Lymphoma Myeloma Leuk 2013;13:370–6.
24. Zhou Y, Chen L, Barlogie B, Stephens O, Wu X, Williams DR, et al. High-risk myeloma is associated with global elevation of miRNAs and overexpression of EIF2C2/AGO2. Proc Natl Acad Sci U S A 2010;107:7904–9.
25. Tsang J, Zhu J, van Oudenaarden A. MicroRNA-mediated feedback and feedforward loops are recurrent network motifs in mammals. Mol Cell 2007;26:753–67.
26. Koeneke E, Witt O, Oehme I. HDAC family members intertwined in the regulation of autophagy: a druggable vulnerability in aggressive tumor entities. Cells 2015;4:135–68.
27. Campbell RA, Sanchez E, Steinberg J, Shalitin D, Li ZW, Chen H, et al. Vorinostat enhances the antimyeloma effects of melphalan and bortezomib. Eur J Haematol 2010;84:201–11.
28. Malumbres M.miRNAs and cancer: an epigenetics view. Mol Aspects Med 2013;34:863–74.
29. Garzon R, Liu S, Fabbri M, Liu Z, Heaphy CE, Callegari E, et al. MicroRNA-29b induces global DNA hypomethylation and tumor suppressor gene reexpression in acute myeloid leukemia by targeting directly DNMT3A and 3B and indirectly DNMT1. Blood 2009;113:6411–8.
30. Liu S, Wu LC, Pang J, Santhanam R, Schwind S, Wu YZ, et al. Sp1/NFkappaB/HDAC/miR-29b regulatory network in KIT-driven myeloid leukemia. Cancer Cell 2010;17:333–47.
31. Fabbri M, Garzon R, Cimmino A, Liu Z, Zanesi N, Callegari E, et al. MicroRNA-29 family reverts aberrant methylation in lung cancer by targeting DNA methyltransferases 3A and 3B. Proc Natl Acad Sci U S A 2007;104:15805–10.
32. Parra M.Class IIa HDACs - new insights into their functions in physiology and pathology. FEBS J 2015;282:1736–44.
33. Kao GD, McKenna WG, Guenther MG, Muschel RJ, Lazar MA, Yen TJ. Histone deacetylase 4 interacts with 53BP1 to mediate the DNA damage response. J Cell Biol 2003;160:1017–27.
34. Mottet D, Pirotte S, Lamour V, Hagedorn M, Javerzat S, Bikfalvi A, et al. HDAC4 represses p21(WAF1/Cip1) expression in human cancer cells through a Sp1-dependent, p53-independent mechanism. Oncogene 2009;28:243–56.
35. Wilson AJ, Byun DS, Nasser S, Murray LB, Ayyanar K, Arango D, et al. HDAC4 promotes growth of colon cancer cells via repression of p21. Mol Biol Cell 2008;19:4062–75.
36. Zhang J, Yang Y, Yang T, Liu Y, Li A, Fu S, et al. microRNA-22, downregulated in hepatocellular carcinoma and correlated with prognosis, suppresses cell proliferation and tumourigenicity. Br J Cancer 2010;103:1215–20.
37. Stronach EA, Alfraidi A, Rama N, Datler C, Studd JB, Agarwal R, et al. HDAC4-regulated STAT1 activation mediates platinum resistance in ovarian cancer. Cancer Res 2011;71:4412–22.
38. Qian DZ, Kachhap SK, Collis SJ, Verheul HM, Carducci MA, Atadja P, et al. Class II histone deacetylases are associated with VHL-independent regulation of hypoxia-inducible factor 1 alpha. Cancer Res 2006;66:8814–21.
39. Jagannathan S, Vad N, Vallabhapurapu S, Vallabhapurapu S, Anderson KC, Driscoll JJ. MiR-29b replacement inhibits proteasomes and disrupts aggresome+autophagosome formation to enhance the antimyeloma benefit of bortezomib. Leukemia 2015;29:727–38.
40. Mithraprabhu S, Kalff A, Chow A, Khong T, Spencer A. Dysregulated Class I histone deacetylases are indicators of poor prognosis in multiple myeloma. Epigenetics 2014;9:1511–20.
41. Kikuchi S, Suzuki R, Ohguchi H, Yoshida Y, Lu D, Cottini F, et al. Class IIa HDAC inhibition enhances ER stress-mediated cell death in multiple myeloma. Leukemia 2015;29:1918–27.
42. Vallabhapurapu SD, Noothi SK, Pullum DA, Lawrie CH, Pallapati R, Potluri V, et al. Transcriptional repression by the HDAC4-RelB-p52 complex regulates multiple myeloma survival and growth. Nat Commun 2015;6:8428.
43. Fulciniti M, Amodio N, Bandi RL, Munshi M, Yang G, Xu L, et al. MYD88-independent growth and survival effects of Sp1 transactivation in Waldenstrom macroglobulinemia. Blood 2014;123:2673–81.
44. Garzon R, Heaphy CE, Havelange V, Fabbri M, Volinia S, Tsao T, et al. MicroRNA 29b functions in acute myeloid leukemia. Blood 2009;114:5331–41.
45. Sampath D, Liu C, Vasan K, Sulda M, Puduvalli VK, Wierda WG, et al. Histone deacetylases mediate the silencing of miR-15a, miR-16, and miR-29b in chronic lymphocytic leukemia. Blood 2012;119:1162–72.
46. Mims A, Walker AR, Huang X, Sun J, Wang H, Santhanam R, et al. Increased anti-leukemic activity of decitabine via AR-42-induced upregulation of miR-29b: a novel epigenetic-targeting approach in acute myeloid leukemia. Leukemia 2013;27:871–8.
47. Richon VM, Webb Y, Merger R, Sheppard T, Jursic B, Ngo L, et al. Second generation hybrid polar compounds are potent inducers of transformed cell differentiation. Proc Natl Acad Sci U S A 1996;93:5705–8.
48. Vesole DH, Bilotti E, Richter JR, McNeill A, McBride L, Raucci L, et al. Phase I study of carfilzomib, lenalidomide, vorinostat, and dexamethasone in patients with relapsed and/or refractory multiple myeloma. Br J Haematol 2015:171:52–9.
49. Siegel DS, Richardson P, Dimopoulos M, Moreau P, Mitsiades C, Weber D, et al. Vorinostat in combination with lenalidomide and dexamethasone in patients with relapsed or refractory multiple myeloma. Blood Cancer J 2014;4:e202.
50. Loos B, Engelbrecht AM, Lockshin RA, Klionsky DJ, Zakeri Z. The variability of autophagy and cell death susceptibility: unanswered questions. Autophagy 2013;9:1270–85.